

# 1 **Revising Contemporary Heat Flux Estimates for the Lena River, Northern Eurasia**

2 Tananaev N.I.<sup>1\*</sup>, Georgiadi A.G.<sup>2</sup>, Fofonova V.V.<sup>3</sup>

3 <sup>1</sup> Melnikov Permafrost Institute SB RAS, Yakutsk, Russia

4 <sup>2</sup> Institute of Geography RAS, Moscow, Russia; [georgiadi@igras.ru](mailto:georgiadi@igras.ru)

5 <sup>3</sup> Alfred Wegener Institute, Helmholtz Centre for Polar and Marine Research, D-25992,  
6 List, Germany; [vera.fofonova@awi.de](mailto:vera.fofonova@awi.de)

7 \* Corresponding author; [TananaevNI@mpi.ysn.ru](mailto:TananaevNI@mpi.ysn.ru); 36 Merzlotnaya Str., Yakutsk, Sakha  
8 (Yakutia) Republic, Russia, 677010

## 9 **Abstract**

10 The Lena River heat flux affects the Laptev Sea hydrology. Published long-term  
11 estimates range from 14.0 to 15.7 EJ·a<sup>-1</sup>, based on data from Kyusyur, at the river outlet.  
12 A novel daily stream temperature ( $T_w$ ) dataset was used to evaluate contemporary Lena  
13 R. heat flux, which is 16.4±2.7 EJ·a<sup>-1</sup> (2002-2011), confirming upward trends in both  $T_w$   
14 and water runoff. Our field data from Kyusyur, however, reveal a significant negative  
15 bias, -0.8°C in our observations, in observed  $T_w$  values from Kyusyur compared to cross-  
16 section average  $T_w$ . Minor Lena R. tributaries discharge colder water during July-  
17 September, forming a cold jet affecting Kyusyur  $T_w$  data. Major  $T_w$  negative peaks  
18 mostly coincide with flood peaks on the Yeremeyka R., one of these tributaries. This  
19 negative bias was accounted for in our reassessment. Revised contemporary Lena R. heat  
20 flux is 17.6±2.8 EJ·a<sup>-1</sup> (2002-2011), and is constrained from above at 26.9 EJ·a<sup>-1</sup> using  
21 data from Zhigansk, ca 500 km upstream Kyusyur. Heat flux is controlled by stream  
22 temperature in June, during freshet period, while from late July to mid-September, water  
23 runoff is a dominant factor.

24 **Keywords:** permafrost hydrology; Russian Arctic; the Lena river; stream temperature;  
25 heat flux

## 26 **Introduction**

27 The terrestrial and marine compartments of the global system are connected via material  
28 and energy fluxes (Huntley *et al.* 2009). In this view, rivers act as major links between  
29 continents and oceans, discharging water and delivering associated fluxes to the coastal  
30 zone. In the Arctic, the largest rivers bear an important thermal imprint on the adjacent  
31 Arctic Ocean regions (Francis *et al.* 2009). Flowing from south to north, they are  
32 immense heat conveyor belts affecting sea water temperature, ice conditions and general  
33 water circulation in the Arctic and North Atlantic (Nummelin *et al.* 2016). Terrestrial  
34 runoff to the Laptev Sea during summer months allows important heat accumulation in  
35 the pycnocline, that affects the thermal state of submarine permafrost (Golubeva *et al.*  
36 2015) and retards ice formation in autumn by 5-6 days (Kirillov 2006). Significant sea ice  
37 production in the Laptev Sea compared to total Arctic Ocean ice budget and a direct link  
38 between warm freshwater input and ice formation (Dmitrenko *et al.* 2009; Gutjahr *et al.*  
39 2016) both add importance to the correct heat flux estimates.

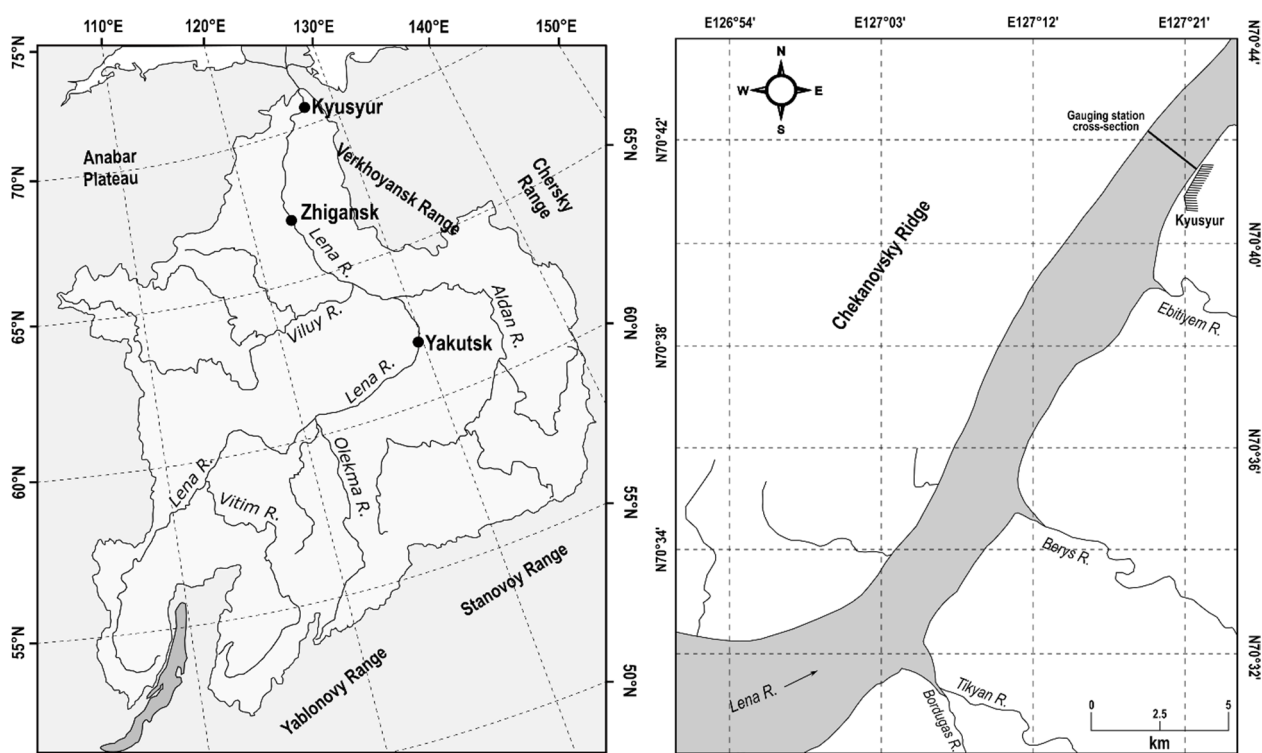
40 Heat flux/runoff is a product of water discharge  $Q$  and stream temperature  $T_w$  hence it  
41 can be affected by changes in both hydrologic and thermal regime under contemporary  
42 climate change (van Vliet *et al.* 2013; Park *et al.* 2017). Recently, numerous studies have  
43 been focusing on hydrologic change in large Arctic catchments (St. Jacques & Sauchyn  
44 2009; Yang *et al.* 2015; Tananaev *et al.* 2016; Georgiadi *et al.* 2017) and riverine heat  
45 flux assessment in its potential relation to global change (Yang *et al.* 2005, 2014;  
46 Lammers *et al.* 2007; Lui & Yang 2011; Fofonova *et al.* 2017; Magritsky *et al.* 2017).

47 Published mean annual heat flux estimates of the Lena R. vary from 14.03 EJ·a<sup>-1</sup> (1950-  
48 1990; Liu & Yang 2011) to 15.2 to 15.7 EJ·a<sup>-1</sup> (1935-2012; Lammers *et al.* 2007;  
49 Georgiadi *et al.* 2017; Magritsky *et al.* 2017). The accuracy of these estimates relies on  
50 the data availability from long-term observation network and the quality of these data.  
51 Daily  $T_w$  data are mostly unavailable for Russian rivers; hence all previous estimates  
52 were based on 10-day averages, that could introduce averaging bias. Moreover, multiple  
53 concerns were expressed since 1930s that  $T_w$  data from Kyusyur GS are negatively biased  
54 because of cold water jet occurring along the right bank in the gauge cross-section  
55 (Reinberg 1938). Modeling-based analysis performed by Fofonova *et al.* (2017) supports  
56 these concerns and casts doubts on the representativeness of the stream temperature data  
57 collected at Kyusyur GS. Their modeling exercises suggest observed  $T_w$  at Kyusyur being  
58 *ca.* 0.8°C lower than midstream temperature or cross-section average. These model  
59 outputs, as well as previous discussion on the matter, lack direct field-based proof. Based  
60 on these conclusions, Magritsky *et al.* (2017) tweak their heat flux estimate from 15.59 to  
61 16.59 EJ·a<sup>-1</sup> to account for potential negative bias in the Kyusyur GS  $T_w$  data, but this  
62 1.0 EJ·a<sup>-1</sup> increase lacks any justification in their paper.

63 This paper employs a daily  $T_w$  dataset at Kyusyur GS (2002-2011; Fofonova *et al.* 2017)  
64 to evaluate mean annual heat flux from daily and 10-day average data and to compare  
65 these values in search for potential averaging bias. Field data from our 2018 observations  
66 of stream temperature distribution in the Kyusyur GS cross-section are used to ‘ground-  
67 truth’ the existence of a cold near-bank jet and its effect on  $T_w$  values measured at the  
68 gauge cross-section. Contemporary heat flux of the Lena R. is then reevaluated based on  
69 daily  $T_w$  values and several thermal regime scenarios, and is constrained from top with  
70 heat flux estimate at Zhigansk GS, *ca.* 500 km upstream Kyusyur.

71 **Study site**

72 The Lena River, with basin area at the outlet *ca.*  $2.43 \cdot 10^6$  km<sup>2</sup>, drains vast areas of  
73 Eastern Siberia from Lake Baikal and Transbaikalia to Anabar Plateau and west slopes of  
74 the Verkhoyansk Range, and enters the Laptev Sea forming the largest delta in the Arctic  
75 (Fig. 1, left). Its mean annual runoff at the outlet equals 575 km<sup>3</sup> (2002-2011), and is  
76 increasing in recent decades (e.g., Tananaev *et al.*, 2016). The catchment is almost  
77 entirely underlain by permafrost, either continuous or discontinuous (Zhang *et al.*, 1999).



79 **Fig. 1** The Lena R. basin (left) and Kyusyur GS location within the Lena R. valley (right)

80 Long-term hydrological monitoring at the Lena R. outlet is performed at Kyusyur, at a  
81 gauging station operated by Russian Hydrometeorological Agency (Roshydromet) since  
82 1935 to present (Fig. 1, right). The Lena R. flows here in a single channel about 2.5 km  
83 wide. The left bank is high and rocky, a minor spur of the Chekanovsky Ridge with  
84 elevation from 200 to 300 m a.s.l., dissected by numerous water tracks and several minor

85 river valleys. The right bank is an alluvial terrace rising gently toward the Kharaulakh  
86 Ridge, a northernmost spur of the Verkhoyansk Range, where elevations range from 500  
87 to 800 m. Numerous minor tributaries flow into the Lena R. from the right (Fig. 1, right),  
88 all draining the westward slope of the Verkhoyansk Range.

89 The Kyusyur gauging station is located within the settlement limits, on the right bank of  
90 the Lena R., and is equipped with a pile water stage gauge. The gauging station is  
91 presently active, but open-access publication of the station data had ceased in 2012.

## 92 **Materials and methods**

93 This study is based on a daily stream temperature  $T_w$  dataset at Kyusyur GS, spanning  
94 from 2002 to 2011 and presented by Fofonova *et al.* (2017). This dataset originates from  
95 Tiksi Branch of Yakutian Hydrometeorological Centre, regional division of Russian  
96 Hydrometeorological Agency (Roshydromet). These data are used to: (a) calculate annual  
97 heat fluxes based on daily  $T_w$  and water discharge data; (b) compare these results with  
98 estimates based on 10-day  $T_w$  averages; (c) revise contemporary heat flux estimates.

99 On the Roshydromet network,  $T_w$  is measured twice daily at 8am and 8pm, near the bank,  
100 using a standard mercury thermometer with a cup-protected bulb to eliminate thermal  
101 inertia on reading. The thermometer is left submerged for at least 5min, then a reading is  
102 taken with 0.1°C accuracy upon thermometer retrieval. Stream temperature is measured  
103 daily but is only published as 10-day averaged values, and raw observed data are virtually  
104 inaccessible for the scientific community. Therefore, most heat flux estimates for Russian  
105 rivers are products of mean 10-day  $T_w$  and water discharge values (e.g. Lammers *et al.*,  
106 2007; Magritsky *et al.*, 2017).

107 The ArcticGRO  $T_w$  data, collected in Zhigansk, *ca.* 500 km upstream Kyusyur (Holmes *et*  
108 *al.*, 2018), are used in the analysis. These data are obtained using the same technique as  
109 described above, but are collected bi-monthly and refer to the temperature at the moment  
110 of observations, and not a daily average. Monthly averages were calculated from  
111 observed values, and heat flux was estimated based on these averages.

112 Daily water discharge  $Q$  data are essential for the heat flux calculations. This study uses  
113 daily  $Q$  values at two gauging stations, Lena R. at Kyusyur and Yeremeyka R. at  
114 Kyusyur, provided by Tiksi Branch of Yakutian Hydrometeorological Centre. Daily  $Q$   
115 values, reported by Roshydromet offices, are not observed directly, but recalculated from  
116 long-term ‘stage-discharge’ curves. Water stage is observed twice daily at 8am and 8pm  
117 at pile water stage gauges at both gauging stations in question. A graduated steel rod is  
118 used to obtain water level reading relative to a closest submerged pile top, which is  
119 translated to water stage (above local datum) and used in water discharge calculation.  
120 The accuracy of long-term stage-discharge curves is estimated to be within 5%.

121 Riverine heat flux/runoff  $HF$ , J, is calculated as:

$$122 \quad HF = C_p \cdot \rho \cdot Q \cdot T_w \cdot n \cdot t, \quad (1)$$

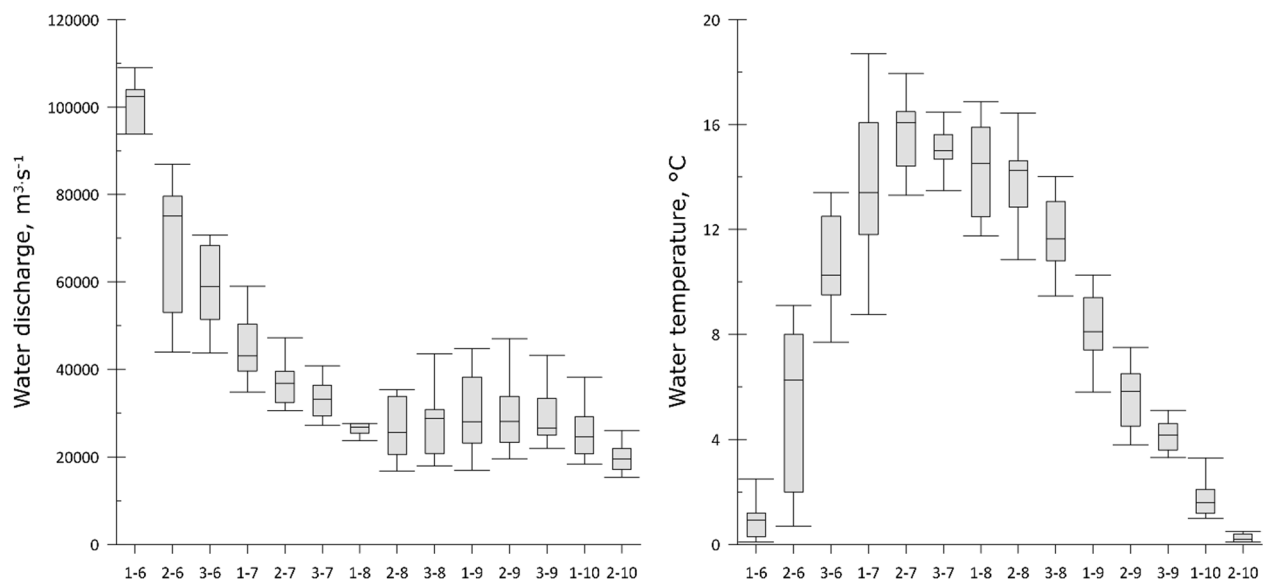
123 where  $C_p$  is specific heat of water, generally variable with temperature but kept constant  
124 at  $4186 \text{ J}\cdot\text{kg}^{-1}\cdot\text{K}^{-1}$  throughout this study;  $\rho$  is water density,  $1000 \text{ kg}\cdot\text{m}^{-3}$ ,  $Q$  is water  
125 discharge,  $\text{m}^3\cdot\text{s}^{-1}$ ;  $T_w$  is stream temperature,  $^{\circ}\text{C}$ ;  $n$  is number of days in the calculation  
126 interval;  $t = 86400$  seconds in a day. Statistical calculations were done in RStudio (2019),  
127 an integrated development environment for R language, using function *groupwiseMean()*,  
128 package ‘rcompanion’ (Mangiafico, 2019).

129 Field data on stream water temperature distribution were collected in Kyusyur in mid-  
130 August 2018, on the falling limb of a major rain-induced flood event originating from the  
131 southern part of the Lena River basin. In the field, water temperature was measured from  
132 a boat with an EXO-2 multiparameter sonde equipped with an internal temperature  
133 sensor, accurate to 0.1°C with 0.01°C resolution, and a pressure/depth sensor. The sonde  
134 was used to observe water temperature at various depths along seven transects at the  
135 gauging station cross-section, and one longitudinal transect extending from the  
136 Ebitiyem R. mouth to the Lena R. right bank (Fig. 1, right).

## 137 **Results**

### 138 *The Lena River $T_w$ and heat flux, 2002-2011*

139 The open-water period at the Lena R. outlet starts around early June. The stream  
140 temperature rises above 0.2°C several days before the ice breakup, on 2 June (average,  
141 2002-2011). At this moment, water discharge peaks, exceeding 100 000 m<sup>3</sup>·s<sup>-1</sup> (Fig. 2,  
142 left). Both  $Q$  and  $T_w$  vary greatly at the falling limb of the freshet, affecting the variability  
143 in resulting heat fluxes. The spring freshet signal fades away by mid-July. Low-flow  
144 period ends by mid-August, then water discharge oscillates until freeze-up because of  
145 numerous rain floods originating from the Lena R. headwaters.



146

147 **Fig. 2** Water discharge and stream temperature of the Lena R. at Kyusyur by 10-day periods. On  
 148 x-axis, 10-day period numbers and months, separated by a hyphen. Boxplots mark median, 25%  
 149 and 75% quartiles, and whiskers match interquartile range x 1.5

150 Stream temperature reaches its maximum values, between 14°C and 16°C on average, by  
 151 early to mid-July, then remains at this plateau until mid-August, and gradually decreases  
 152 to 0.2°C by mid-October (Fig. 2, right). Mean highest daily  $T_w$  is  $18.5 \pm 1.5^\circ\text{C}$  and is  
 153 observed in July. Multiple publications claim upward trends in  $T_w$  in recent decades  
 154 (Yang *et al* 2005; Liu & Yang 2011; Georgiadi *et al* 2017; Magritsky *et al* 2017); our  
 155 results support these conclusions.

156 In numerous preceding publications, heat flux of the Lena R. at Kyusyur GS is assessed  
 157 using published 10-day averages (1935-2012; Georgiadi *et al.* 2017; Lammers *et al.*  
 158 2007; Magritsky *et al.* 2017). Here, the daily  $T_w$  dataset is used in calculations along with  
 159 10-day averages; Eq. 1 was used in calculations. Data analysis reveals no averaging bias  
 160 related to the use of 10-day average  $T_w$  in lieu of daily values, the two estimates being  
 161 identical at  $16.4 \pm 2.7 \text{ EJ} \cdot \text{a}^{-1}$ . This is substantially higher than previous estimates, and is  
 162 close to  $16.04 \text{ EJ} \cdot \text{a}^{-1}$  estimate for 1980-2012, published by Magritsky (2016).



164 Besides averaging bias, the  $T_w$  data from Kyusyur GS are reported to be negatively  
 165 biased, affected by a cold jet in the near-bank zone (Reinberg 1938). Our field data from  
 166 the 2018 campaign confirm this report.

167 Water temperature distribution at the Kyusyur GS cross-section is found to be mostly  
 168 uniform in both vertical (surface to bottom) and lateral (bank to bank) directions. Vertical  
 169 temperature distribution is uniform at least in the first 7 to 10 m of the water column,  
 170 evidencing strong turbulent mixing in the cross-section, reserve observation points  
 171 adjacent to riverbanks (Table 1, Fig. 3). At Transect 1, near the left bank, water  
 172 temperature decreases with depth by only  $0.18^\circ\text{C}$  within 10 m, while at Transect 7, along  
 173 the right bank, several distinct water masses are observed, the one at 4 m depth having  
 174 properties resembling those of the surface waters (Fig. 3, right).

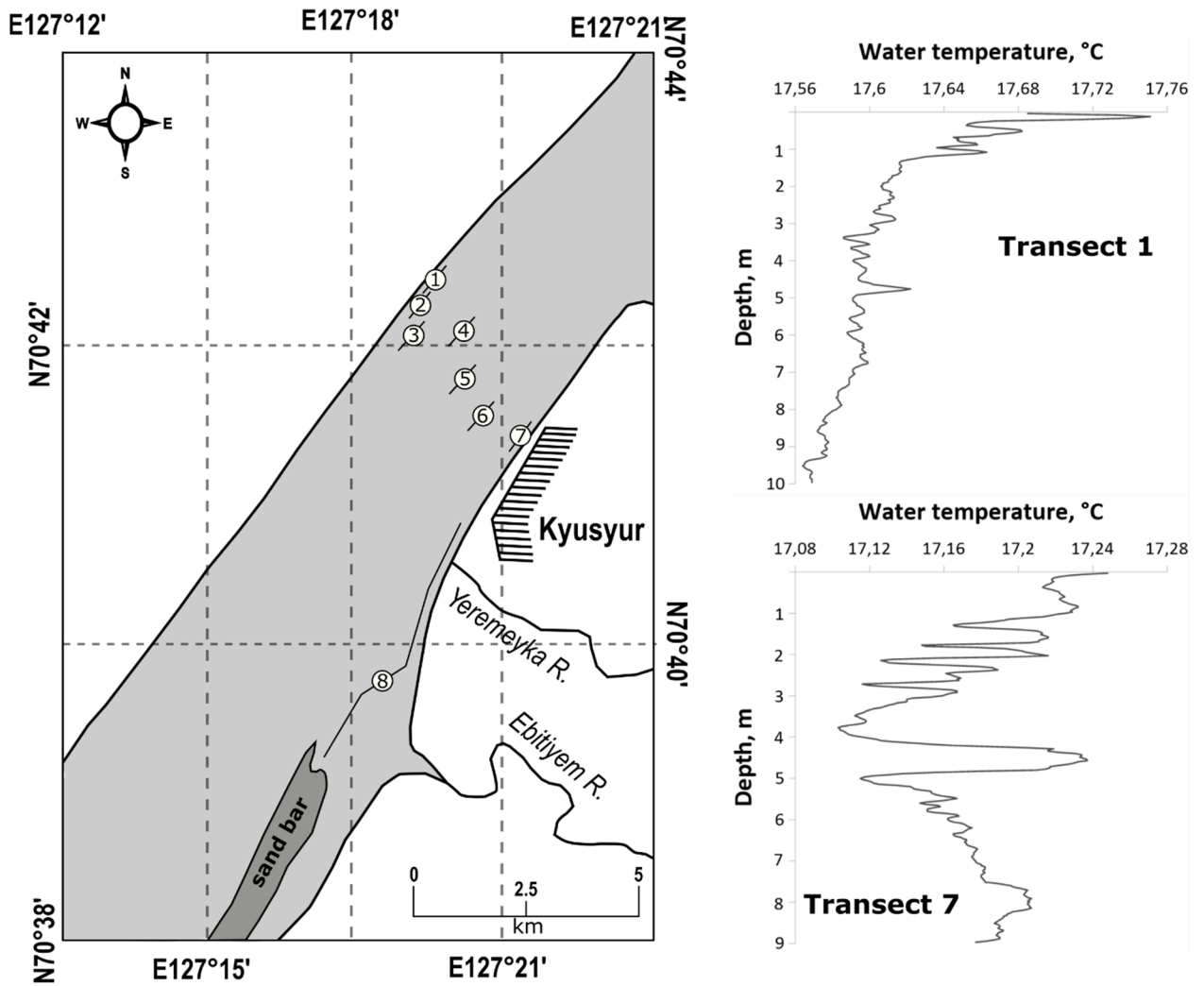
175 **Table 1**  
 176 Water temperature of the Lena R. at transects in the Kyusyur GS cross-section (see Fig. 3 for  
 177 spatial reference; observations made 15 August 2018)

178

Transect	Depth $d$ , m	Surface $T_w$ , $^\circ\text{C}$	$T_w$ at depth $d$ , $^\circ\text{C}$	Mean $T_w$ , $^\circ\text{C}$
1	10	17.75	17.57	17.6
2	7	17.76	17.76	17.76
3	7	17.84	17.82	17.83
4	7	17.9	17.9	17.9
5	8	18.0	17.98	18.0
6	9	17.9	17.88	17.9
7	9	17.2	17.1	17.15

179

180 In lateral direction, lower temperature values were observed near the banks of the  
 181 Lena R. Midstream water temperature was around 17.9 to 18.0°C, but it was by 0.4°C  
 182 lower at Transect 1, and by 0.85°C lower at Transect 7 (Table 1). Thermal impact of  
 183 minor tributaries, heat exchange with channel bottom, cooling influence of permafrost or  
 184 stream circulation patterns may be deemed responsible for these anomalies.

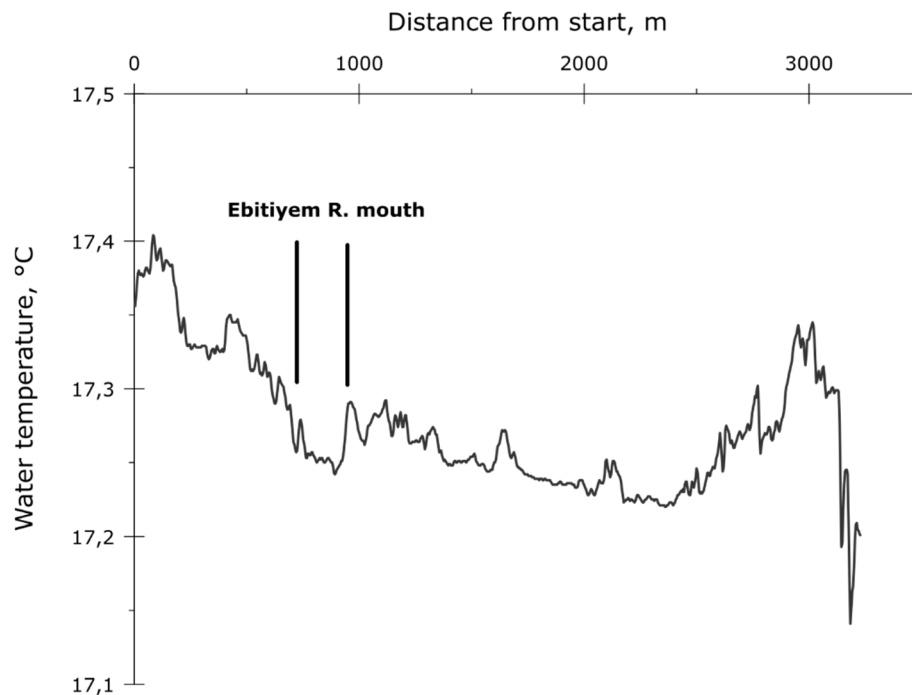


185

186 **Fig. 3** Water temperature observation points near Kyusyur GS (left), vertical temperature  
 187 profiles at near-bank transects (right)

188 Numerous minor mountainous tributaries drain to the Lena R. along the right bank of the  
 189 river (see Fig. 1, right). Their potential impact on the Lena R. thermal regime and their  
 190 role in producing this relatively cold jet along the right bank of the river have been

191 demonstrated previously (Fofonova *et al.*, 2017), though other explanations cannot be  
192 ruled out straight away and are discussed further in the text. A transect was then planned  
193 to track longitudinal gradient in water temperature around the mouth zone of such  
194 tributaries. The closest tributary upstream from Kyusyur is the Yeremeyka R. (Fig. 3,  
195 left), but it had completely dried out at the time of our fieldwork. Observations were then  
196 performed at the mouth of a larger river, the Ebitiyem R., from a moving boat with a  
197 sensor submerged at *ca.* 0.5 m depth. Data from this longitudinal transect between the  
198 Ebitiyem R. mouth to the Lena R. right bank, confirm that thermal imprint of this  
199 tributary is significant and persists at least as far as the gauging station area (Fig. 4).



200

201 **Fig. 4** The Lena R. surface water temperature along the Transect 8, see Fig. 3, right, for

202

reference

203 Upstream the tributary mouth, water was already cooler than at midstream, *ca.* 17.4°C,

204 and a further decrease down to 17.2°C is corresponding to the tributary inflow. This

205 pattern continues toward the gauging station, where water temperature drops further to

206 17.1°C (Fig. 4). A 1.5°C decrease in water temperature toward the end of the transect  
207 was observed where the survey boat approached the right bank and was about 100 m  
208 from the shoreline.

209 Field results prove the incoherence of the  $T_w$  data reported by Kyusyur GS, with the  
210 temperature difference between midstream and near-bank,  $\Delta T_w$ , reaching 0.85°C.  
211 Discharge-weighted cross-sectional average  $T_w$  is not expected to be significantly lower  
212 than midstream, since ‘colder’ channel sections adjacent to riverbanks are relatively  
213 shallow and have lower velocity. Detailed seasonal surveys are to be performed to relate  
214 observations at Kyusyur GS to cross-section average  $T_w$ .

#### 215 *Scenario-based Lena R. heat flux reassessment*

216 The Lena R. heat flux for the 2002-2011 period was reassessed upon collecting field  
217 evidences that the  $T_w$  values observed at Kyusyur GS are misrepresentative for the cross-  
218 section average. A correction factor  $\Delta T_w$ , either constant or time-dependent, was  
219 introduced in the observed data. Its value cannot be derived from a single field survey,  
220 hence modeling results presented in (Fofonova *et al.*, 2017) were used in scenario  
221 building. These referenced results were output from a numerical experiment, performed  
222 using a Computational Fluid Dynamics module in COMSOL Multiphysics®, a modeling  
223 software platform for finite-element analysis.

224 Two simple hypothetical scenarios were developed, for constant or time-dependent  $\Delta T_w$ .  
225 For all scenarios,  $\Delta T_w = 0^\circ\text{C}$  for May, June and October.

226 Scenario 1:  $\Delta T_w = +0.8^\circ\text{C}$  for July, August and September. This  $\Delta T_w$  value is a simulated  
227 mean difference between cross-section average  $T_w$  and near-bank  $T_w$  observed at Kyusyur  
228 GS (Fofonova *et al.*, 2017, Fig. 9a), and is surprisingly close to our field results. This

229 correction increases the Lena R. heat flux to  $17.3 \pm 2.8 \text{ EJ}\cdot\text{a}^{-1}$  (2002-2011) *i.e.* by 5%  
230 compared to uncorrected value.

231 Scenario 2: is based on the previous scenario, but accounts for extreme temperature  
232 gradients that could be observed throughout the open-water period. Simulated daily  $\Delta T_w$   
233 values were up to +3.0°C in July 2011 and August 2007, and up to +5°C in September  
234 2003 on certain days (Fofonova *et al.* 2017). Highest monthly average  $\Delta T_w$  values were  
235 +2.0°C in July and August, and +3.0°C in September.

236 Monthly  $\Delta T_w$  variation scenarios were formulated as follows, allowing temperature  
237 anomalies in one of three months (Cases 2-4), two (Cases 5-7) or in all three months  
238 (Case 8):

239 (1) July-September,  $\Delta T_w = +0.8^\circ\text{C}$ , same as Scenario 1;

240 (2) July,  $\Delta T_w = +2.0^\circ\text{C}$ ; August-September,  $\Delta T_w = +0.8^\circ\text{C}$ ;

241 (3) July & September,  $\Delta T_w = +0.8^\circ\text{C}$ ; August,  $\Delta T_w = +2.0^\circ\text{C}$ ;

242 (4) July & August,  $\Delta T_w = +0.8^\circ\text{C}$ ; September,  $\Delta T_w = +3.0^\circ\text{C}$ ;

243 (5) July & August,  $\Delta T_w = +2.0^\circ\text{C}$ ; September,  $\Delta T_w = +0.8^\circ\text{C}$ ;

244 (6) July,  $\Delta T_w = +2.0^\circ\text{C}$ ; August,  $\Delta T_w = +0.8^\circ\text{C}$ ; September,  $\Delta T_w = +3.0^\circ\text{C}$ ;

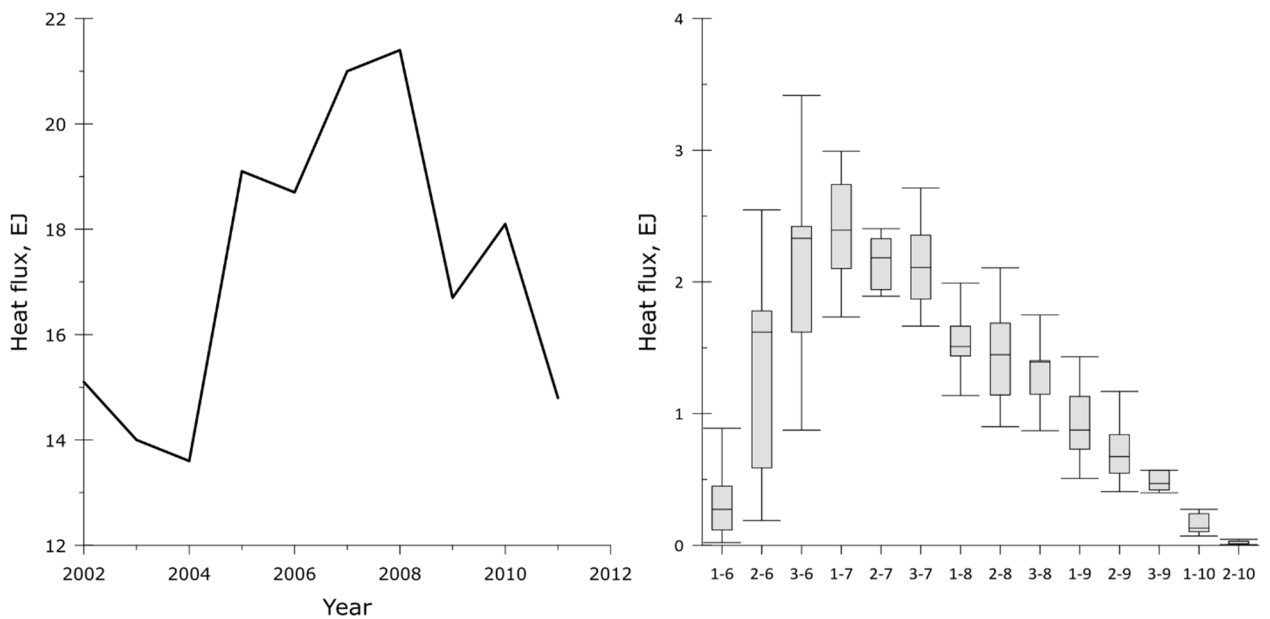
245 (7) July,  $\Delta T_w = +0.8^\circ\text{C}$ ; August,  $\Delta T_w = +2.0^\circ\text{C}$ ; September,  $\Delta T_w = +3.0^\circ\text{C}$ ;

246 (8) July & August,  $\Delta T_w = +2.0^\circ\text{C}$ ; September,  $\Delta T_w = +3.0^\circ\text{C}$ .

247 These distributions have differing frequencies of occurrence, or return periods, which are  
248 unknown for general population. Sample frequencies, calculated based on modeling  
249 results from Fofonova *et al.* (2017), were used in further analysis. Cases 2-4 each occur  
250 once in 10 years, as they were each observed once during the decadal modeling interval.  
251 Cases 5-7 occur once in 100 years, and Case 8 once in 1000 years, as per joint probability

252 calculation rules. Case 1 takes what is left, or 889 years out of 1000. Heat fluxes were  
 253 calculated for each year of record and for each case, then this dataset was bootstrapped  
 254 with number of permutations  $n = 10000$  accounting for frequencies of occurrence.  
 255 Revised contemporary mean annual Lena R. heat flux is estimated at  $17.6 \pm 2.8 \text{ EJ}\cdot\text{a}^{-1}$   
 256 (2002-2011; Fig. 5), corrected for  $\Delta T_w$  extremes and accounting for their return periods.

257



258

259 **Fig. 5** Revised annual Lena R. heat flux, 2002-2011, and its distribution across 10-day periods.  
 260 On  $x$ -axis, 10-day period numbers and months, separated by a hyphen. Boxplot marks median,  
 261 25% and 75% quartiles, and whiskers match interquartile range  $\times 1.5$

262 The Lena R. heat flux appears to vary highly across years (Fig. 5). At a monthly scale,  
 263 late June fluxes are highly variable and could mark annual maximum; on average,  
 264 however, the latter is observed in July, when the freshet is still at its falling limb and  
 265 highest  $T_w$  are observed.

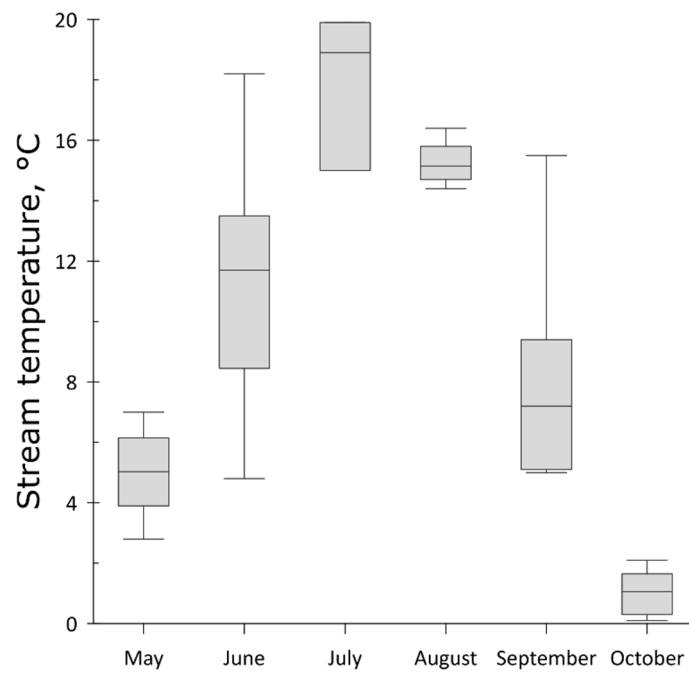
266 **Discussion**

267 *Constraining Lena R. heat flux estimate*

268 The revised estimate is based on modeling results, assuming a virtually constant  $\Delta T_w$   
269 value. Its lower bound constraint can be easily estimated at  $16.4 \text{ EJ}\cdot\text{a}^{-1}$ , *i.e.* estimated heat  
270 flux before temperature corrections. The upper bound constraint is hard to assess based  
271 on data from Kyusyur GS, since the true  $\Delta T_w$  and its temporal variation are unknown.  
272 The ArcticGRO  $T_w$  dataset collected in Zhigansk GS, about 500 km upstream from  
273 Kyusyur, is used to evaluate the upper bound constraint. Water discharge data from  
274 Kyusyur GS are used in calculations, since the gauging station in Zhigansk had never  
275 observed this parameter. A certain positive bias may originate from this substitute, since  
276 the distance between the two gauging stations is significant, and water discharge in  
277 Zhigansk is expected to be somewhat less than in Kyusyur. However, no major tributaries  
278 flow into the Lena R. between the gauging stations in question. The potential increase in  
279 discharge is negligible compared to the Lena R. discharge, though hard to quantify, since  
280 no gauging stations observe the discharge of minor tributaries between Zhigansk and  
281 Kyusyur. Secondly, as we look for the upper bound constraint, this positive bias raising  
282 the upper bound might not be critical for evaluation purposes.

283 In total, ArcticGRO database contains 38  $T_w$  observations from 2003 to 2018, covering  
284 the open water period from mid-May to early October. These observations were averaged  
285 across months (Fig. 6). These are rough estimates since  $T_w$  measurements are unevenly  
286 distributed throughout months, but they are based on the only data which are openly  
287 available. Corresponding mean monthly water discharge values at Kyusyur GS for 2002-  
288 2011 period were used in calculations.

289



290

291 **Fig. 6** Mean monthly stream temperature, the Lena R. at Zhigansk GS, ArcticGRO data (Holmes  
 292 *et al.* 2018)

293 Mean annual heat flux at Zhigansk GS equals  $26.9 \text{ EJ} \cdot \text{a}^{-1}$  (2003 to 2011) and can serve as  
 294 an extreme upper bound to constrain the heat flux observed at Kyusyur GS, supposing  
 295 that total heat turnover in the stream is maintained at zero level as water travels from  
 296 Zhigansk to Kyusyur.

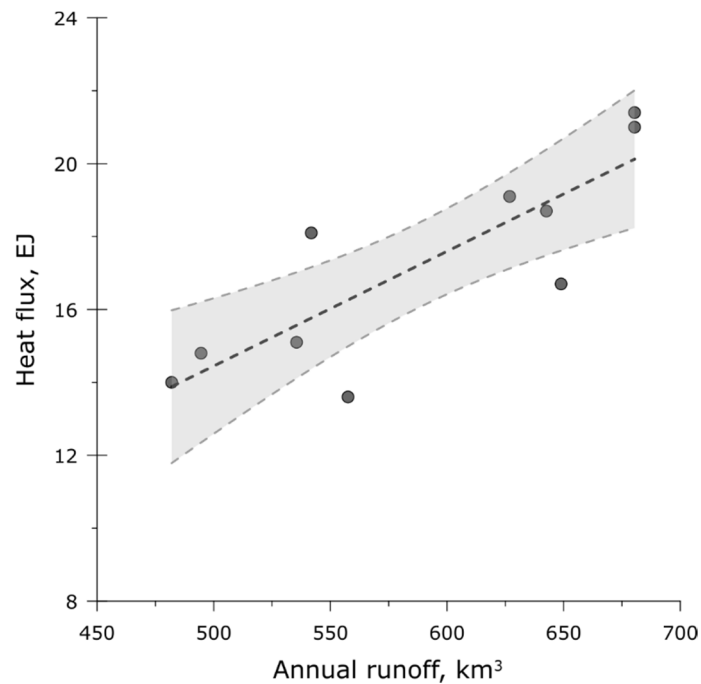
297 *Hydrological controls over the Lena R. heat flux*

298 Riverine heat flux is controlled by water discharge and stream temperature, both highly  
 299 variable. In a long-term perspective, the heat flux variation of the Lena R. is mostly  
 300 related to changes in water runoff (Fig. 7). The following linear equation describes this  
 301 relation ( $r = 0.84, p < 0.01$ ):

302 
$$HF = 0.0315 \cdot W_Q - 1.28, \quad (2)$$

303 where  $HF$  – annual heat flux/runoff, EJ;  $W_Q$  – annual runoff,  $\text{km}^3$ .





305

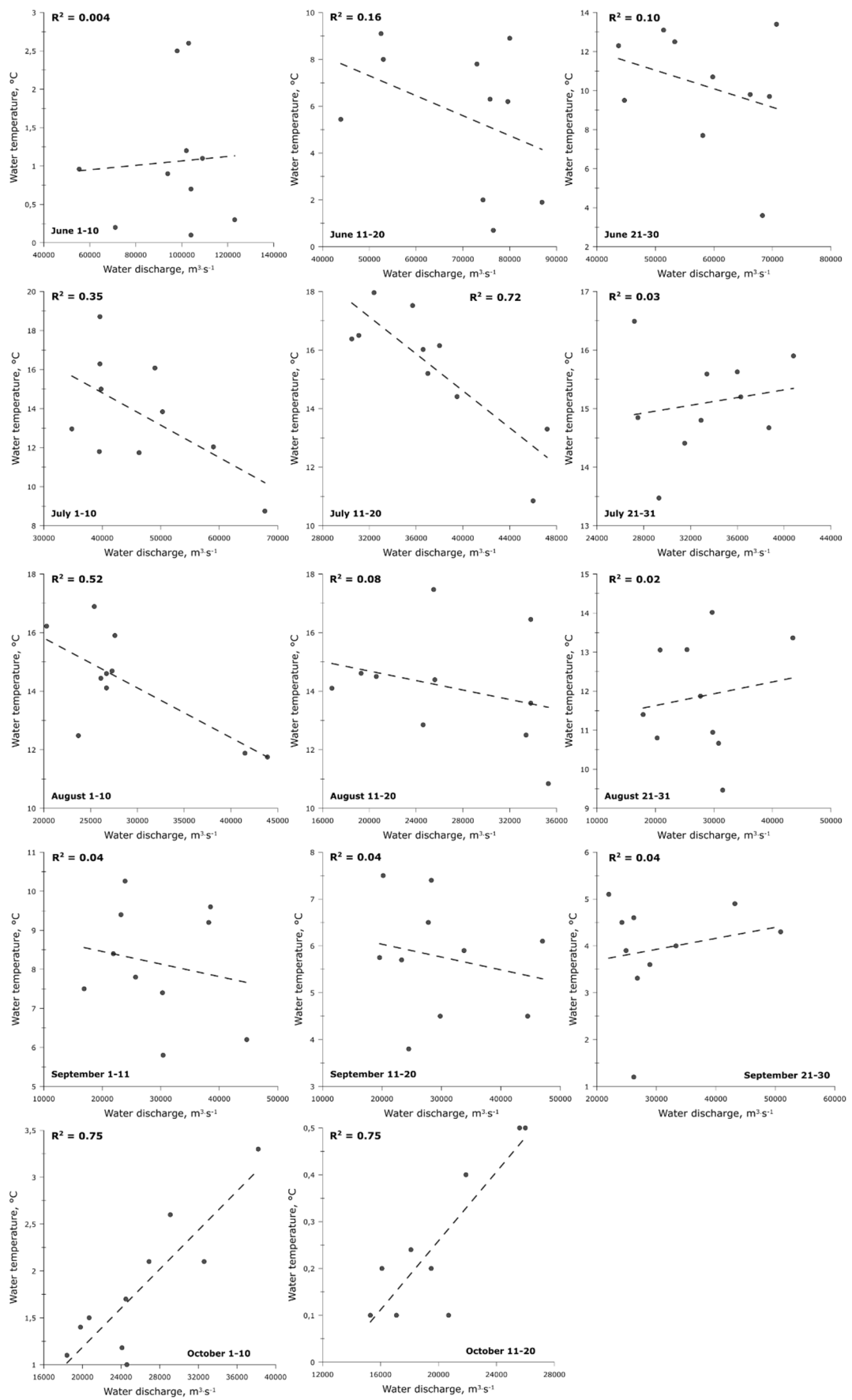
306 **Fig. 7** The Lena R. annual heat flux related to annual runoff at Kyusyur GS, 2002-2011

307 However, at sub-annual scale, water discharge and stream temperature seem to mostly act  
 308 as two independent controls over heat flux. For most of the year, these two parameters  
 309 are mutually independent at a 10-day scale at  $R^2$  below 0.2, with a slight tendency toward  
 310 lower  $T_w$  values at higher discharges (Fig. 8). Notable exceptions include early and mid-  
 311 July, when  $T_w$  is decreasing with higher  $Q$  ( $R^2 = 0.35...0.72$ ) and October, when this  
 312 same relation is positive with  $R^2 = 0.75$ .

313 Falling limb of a freshet generally continues to mid-July, and high discharge at this time  
 314 corresponds to the overlapping rain events. The latter originate from the mountainous  
 315 southern part of the basin, where permafrost groundwater and numerous icings may  
 316 influence stream temperature. However, their thermal impact is expected to be negligible,  
 317 as this water should accumulate heat during its 2000 km descent to Kyusyur. Hence  
 318 closer sources are to be thought of. The Vilyui R. is regulated by a large hydropower

319 station, discharging colder waters, but its water temperature returns to equilibrium values  
320 by the river mouth (Magritsky, 2016). The retarded freshet or juxtaposed rain floods on  
321 the Aldan River (Fig. 1, left) could be responsible for this temperature decline. Most of  
322 its basin is mountainous, where icings are abundantly present, and flash floods are  
323 common on its right tributaries upstream the Lena-Aldan confluence.

324 In October, higher runoff is also related to rain events, but at this time, the most distant  
325 sources of warmer water are at play. Longer travel time assures higher heat accumulation  
326 may be partly related to heat release from the alluvial channel and floodplain. The Lena  
327 R. channel between Yakutsk and Zhigansk accommodates enormous sand bars, that are  
328 drained and exposed to sunlight at low levels. Their prolonged inundation toward the end  
329 of autumn might serve an important heat source, as previously suggested by Fofonova *et*  
330 *al* (2017), though never assessed directly.



331

332

**Fig. 8** The Lena R. water discharge related to 10-day average  $T_w$ , Kyusyur GS (2002-2011)

333 When water discharge and temperature are correlated, both are controlling heat flux.  
 334 When no relation is observed, both fluctuate chaotically and none has a unique control on  
 335 heat flux. However, two distinct periods with both  $Q$ -controlled and  $T_w$ -controlled heat  
 336 flux emerge in our analysis. Temperature-controlled heat flux is observed throughout  
 337 June, while most of the open-water period the Lena R. heat flux is discharge-controlled  
 338 (Table 2).

339 **Table 2**  
 340 Discharge- vs water temperature-controlled heat flux periods, the Lena R. at Kyusyur  
 341

Period	$R^2, Q$ vs HF	$R^2, T_w$ vs HF	Pattern
June 1-10	0.04	<b>0.98</b>	$T_w$ -controlled
June 11-20	$3 \cdot 10^{-5}$	<b>0.83</b>	$T_w$ -controlled
June 21-30	0.07	<b>0.68</b>	$T_w$ -controlled
July 1-10	0.15	0.24	
July 11-20	0.12	0.04	
July 21-31	<b>0.91</b>	0.22	$Q$ -controlled
August 1-10	<b>0.80</b>	0.12	$Q$ -controlled
August 11-20	<b>0.69</b>	0.08	$Q$ -controlled
August 21-31	<b>0.85</b>	0.27	$Q$ -controlled
September 1-10	<b>0.66</b>	0.16	$Q$ -controlled
September 11-20	<b>0.72</b>	0.11	$Q$ -controlled
September 21-30	<b>0.77</b>	<b>0.41</b>	
October 1-10	<b>0.86</b>	<b>0.96</b>	
October 11-20	<b>0.87</b>	<b>0.96</b>	

342 Values in **bold** are significant at  $p < 0.01$

343 This apparent seasonality stems from this large river hydrology. During the freshet, water  
344 discharge is enormously high, occasionally exceeding  $150\,000\text{ m}^3\cdot\text{s}^{-1}$ , and even slightly  
345 warmer water will produce disproportionately high HF response compared to other  
346 periods. From the end of July to late September, the variation in  $T_w$  decreases since the  
347 major heat source across the basin is solar radiation (see Fig. 2, right), and the amount of  
348 water takes over the total heat flux value for these periods.

349 This pattern has long-standing implications from the climate change perspective. We can  
350 assume that climate change effects on the Lena R. heat flux would be less significant if  
351 they will be related to: (a) water discharge increase in June, *e.g.* higher snow water  
352 equivalent during winter or higher rainfall around the freshet peak; (b) water temperature  
353 increase in August-September, *e.g.* persistent high pressure over central Yakutia or less  
354 impact from cooler mountainous rivers. In contrast, (c) an increase in June water  
355 temperature, associated with earlier onset of summer, or (d) rainfall runoff increase  
356 throughout July and August, caused by heavy rains in the Vitim and Olyokma R. basins,  
357 will lead to pronounced heat flux increase in Kyusyur and in the Lena Delta region. In all  
358 cases, runoff/temperature increase in October will lead to higher heat flux.

#### 359 *Cold water origin in the Lena R. channel*

360 Thermal impact of minor tributaries, heat exchange with channel bottom, cooling  
361 influence of permafrost or stream circulation patterns may be deemed responsible for an  
362 observed negative temperature anomaly at the Kyusyur GS. Heat exchange with channel  
363 bottom is expected to be negligible, compared to total heat export of the Lena R., because  
364 of the presence of a talik, or an extensive non-frozen zone below the channel. Thermal  
365 regime of this talik zone is controlled by convective heat transfer of riverine waters

366 (Wankiewicz 1984), therefore only minor thermal influence on the near-bottom stream  
367 temperature is expected.

368 Permafrost is present in riverbanks as both frozen soil, ice wedges and massive ground  
369 ice, and its melting can potentially affect the stream temperature. During the low-flow  
370 period, permafrost meltwater drains to the main Lena R. channel as small springlets,  
371 potentially contributing to water temperature decrease. However, this influence might not  
372 extend more than by several meters from the shoreline because of modest volumetric  
373 contribution of these springlets to the total summer runoff.

374 The thermal effect of steady open-channel circulation near Kyusyur GS cannot be  
375 completely ruled out, but even if present, its influence is mostly indirect. The straight  
376 channel segment adjacent to Kyusyur GS (see Fig. 1, right) is an outer part of a Lena R.  
377 channel bend. A steady outer-bank circulation cell is expected to be present in the flow  
378 (Blanckaert & de Vriend 2004), inhibiting lateral mixing. Therefore, contrasting stream  
379 properties in the alongshore river section, including stream temperatures, are in part  
380 secured by this circulation cell. Lateral input from tributaries is expected to be ‘locked’ in  
381 this cell as long as this circulation pattern persists.

382 Previous modeling results (Fofonova *et al.* 2017) and our field observations strongly  
383 support the origin of the cold water jet along the right bank of the Lena R. from  
384 numerous minor right-bank tributaries (Fig. 1, right). While flow may cease during  
385 summer on smaller creeks, like the Yeremeyka R. with basin area of 9.7 km<sup>2</sup>, the larger  
386 tributaries maintain their flow throughout the rain-free period. The thermal impact of  
387 these minor tributaries, already significant under low-flow conditions, may increase  
388 drastically during heavy rains in their basins. This effect was traced in the  $T_w$  data

389 observed at Kyusyur GS, using daily discharge data from the Yeremeyka R. at Kyusyur,  
 390 a gauging station at the outlet of a minor Lena R. tributary (see Fig. 3, left). In most  
 391 cases, the  $T_w$  in Kyusyur drops significantly at the time of the flood peak at the  
 392 Yeremeyka R., which in this analysis represents all minor right tributaries (Table 3). This  
 393 effect is present at various Lena R. discharges, up to  $78100 \text{ m}^3 \cdot \text{s}^{-1}$ . It is less pronounced  
 394 in September, and can exceed  $2.5^\circ\text{C}$  in July (Table 3). These data strongly support the  
 395 origin of the cold near-bank water from numerous minor right-hand tributaries of the  
 396 Lena R.

**Table 3**

397 Thermal effect of the rain flood peaks on the right-bank tributaries, represented by the  
 398 Yeremeyka R., on the Lena R.  $T_w$  at Kyusyur GS, 2002-2011  
 399

Year	Flood peak, Yeremeyka R.		Minimum $T_w$ at Kyusyur			
	Date	$Q, \text{ m}^3 \cdot \text{s}^{-1}$	Date	$Q, \text{ m}^3 \cdot \text{s}^{-1}$	Min $T_w, ^\circ\text{C}$	Off-min $T_w, ^\circ\text{C} (*)$
2002	29.07	2.34	31.07	35400	10.9	11.7
2003	29.07	1.26	30.07	32200	10.9	14.3
	08.09	3.14	09.09	25600	3.9	5.2
2004	30.08	1.22	01.09	30100	7.8	8.0
2005	30.08	1.09	01.09	46200	6.5	7.0
	19.09	0.66	22.09	35200	3.8	3.9
2006	24.07	1.58	24.07	34200	11.5	12.3
	06.08	1.25	06.08	26100	15.5	16.3
	18.09	0.74	–	–	–	–
2007	18.06	1.29	19.06	78100	8.3	9.8
	11.07	1.58	11.07	44400	8.6	11.6
	01.08	2.71	04.08	42300	10.7	11.8
2008	28.08	0.49	–	–	–	–
2009	04.09	0.74	04.09	30800	4.5	5.1
	09.09	0.74	09.09	31200	4.8	5.6

2010	28.06	0.73	–	–	–	–
	27.07	1.51	28.07	40200	14.9	15.2
	01.09	0.45	02.09	22500	10.6	10.8
2011	09.07	0.72	09.07	30000	12.3	13.4
	17.07	1.14	–	–	–	–
	27.07	0.68	29.07	25200	14.8	15.3

400 (\*) Calculated as average  $T_w$  of the two days adjacent to the minimum  $T_w$  date in Kyusyur GS

401 The potential sources of this cold storm- and baseflow are numerous, snow and icings  
402 meltwater, and groundwater flow among the most important.

403 Snow cover in this High Arctic region normally decays by mid-June, but remnant snow  
404 patches may persist until late July and even to mid-August in shadowed valleys, adjacent  
405 to north-facing valley slopes and in the mountainous areas of the Verkhoyansk Range.

406 Thermal impact of melting snow on water temperature during summer months is  
407 probably negligible, since meltwater from these snow patches is not directly connected to  
408 streamflow and has to travel through the floodplain, mostly in the active layer, to reach  
409 the nearby streams.

410 Icings are common permafrost hydrology features (Pinneker, 1990; Yoshikawa *et al.*,  
411 2007). Normally, medium and large icings of the Verkhoyansk region completely decay  
412 by late August, and only the largest ones are capable of surviving one or more summers.  
413 Their contribution to river runoff may reach significant proportions, up to 12% of total  
414 basin discharge (Clark, Lauriol, 1997), particularly important during baseflow period, but  
415 also during heavy rainfall, when the flood wave leads to ice deterioration and decay. Cold  
416 icing water is directly connected to streams and may play a significant role in water  
417 cooling. Several typical icing fields in the Tikyan R. basin are detectable using satellite  
418 imagery.



419 Groundwater flow has minor influence on river runoff in the continuous permafrost  
420 regions, but the presence of icings confirms groundwater discharge in the valleys of  
421 minor Lena R. tributaries. Regional observations on groundwater temperature are absent,  
422 but most springs are reported to have water temperatures close to 0°C under similar  
423 conditions in northeastern Alaska (Kane *et al.*, 2013).

#### 424 *Implications for other Russian Arctic gauging stations*

425 Our results show that local hydrology may interfere severely with the accuracy of routine  
426 stream temperature observations. To this end, data from the major Russian Arctic river  
427 outlets should be analysed for relevance. At the Yenisey R. outlet, stream temperature is  
428 observed at Igarka GS. This gauging station is situated on the right bank of the Igarskaya  
429 Branch, a large side channel receiving numerous tributaries upstream the GS cross-  
430 section. The Ob R. outlet is at Salekhard GS, where the gauging station is situated on the  
431 right bank of a secondary branch in a highly braded section. In theory, the data from  
432 these stations can also be biased and misrepresent the cross-section average  $T_w$ . If this is  
433 the case, then the total heat flux from the Russian Arctic rivers is undervalued, affecting  
434 the quality of ocean circulation model outputs.

#### 435 **Conclusions**

436 This study confirms, with both published and field data, that stream temperature  
437 observations at Kyusyur GS are misrepresentative neither for midstream nor the cross-  
438 sectional average temperatures.

439 During our field survey, the water temperature at the observation point of Kyusyur GS,  
440 *ca.* 3 m from the river bank, was found to be by 0.85°C lower than midstream  
441 temperature, which is surprisingly close to previous modeling results (Fofonova *et al.*,

442 2017). Field data evidence the existence of a relatively cold-water jet extending at least  
443 150 m from the right Lena R. bank toward midstream.

444 We conclude therefore that existing heat flux calculations for the Lena R. at Kyusyur are  
445 negatively biased. The thermal impact of numerous minor upstream tributaries is shown  
446 to be a major reason for this misrepresentation, and to increase during rain floods on  
447 these tributaries.

448 Revised Lena R. heat flux estimate, corrected for this negative bias, is  $17.6 \pm 2.8 \text{ EJ}\cdot\text{a}^{-1}$ .  
449 From the upper bound, our estimate is constrained at  $26.9 \text{ EJ}\cdot\text{a}^{-1}$ , obtained using monthly-  
450 averaged  $T_w$  data from Zhigansk GS, ca. 500 km upstream Kyusyur. During most of the  
451 year, water discharge is controlling heat flux value, but in June, the latter is totally  
452 controlled by stream temperature.

#### 453 **Acknowledgements**

454 This study is partially funded by Russian Fund for Basic Research, Project 17-05-00948  
455 (hydrological analysis and heat flux calculations), Project 18-05-60240-ARCTIC (field  
456 investigations). The authors are grateful to Afanasiy Popov (technician, Kyusyur GS,  
457 Roshydromet) and other locals for the assistance in the 2018 fieldwork.

458 **Author contributions.** Conceptualization, methodology, investigation, formal analysis,  
459 writing – original draft, N.T.; Funding acquisition, conceptualization, investigation, A.G.;  
460 Resources, V.F.; Data curation, N.T. and V.F. All authors contributed to discussions,  
461 review and editing of the original draft.

#### 462 **References**

- 463 Blanckaert K. & de Vriend H.J. (2004) Secondary flow in sharp open-channel bends, *J. Fluid*  
464 *Mech.* **498**, 353–380.
- 465 Clark I.D., Lauriol B. (1997) Aufeis of the Firth River basin, Northern Yukon, Canada: Insights  
466 into permafrost hydrogeology and karst, *Arctic and Alpine Res.* **29(2)**, 240–252.
- 467 Dmitrenko I.A., Kirillov S.A., Tremblay L.B., Bauch D. & Willmes S. (2009) Sea-ice production  
468 over the Laptev Sea shelf inferred from historical summer-to-winter hydrographic observations  
469 of 1960s-1990s, *Geophys. Res. Lett.* **36**, L13605, doi: 10.1029/2009GL038775.
- 470 Fofonova V., Zhilyaev I., Kraineva M., Iakshina D., Tananaev N., Volkova N., Sander L.,  
471 Papenmeier S., Michaelis R. & Wiltshire K.H. (2017) Features of the water temperature long-  
472 term observations on the Lena River at basin outlet, *Polarforschung* **87(2)**, 135-150.
- 473 Francis J.A., White D.M., Cassano J.J., Gutovski Jr. W.J., Hinzman L.D., Holland M.M., Steele  
474 M.A. & Vörösmarty C.J. (2009) An arctic hydrologic system in transition: Feedbacks and  
475 impacts on terrestrial, marine, and human life, *J. Geophys. Res.* **114**, L04019, doi:  
476 10.1029/2008JG000902.
- 477 Georgiadi A.G., Kashutina E.A. & Milyukova I.P. (2017) Long-term changes of water flow,  
478 water temperature and heat flux of the largest Siberian rivers, *Polarforschung* **87(2)**, 167-176.
- 479 Golubeva E., Platov G., Malakhova V., Iakshina D. & Kraineva M. (2015) Modeling the impact  
480 of the Lena River on the Laptev Sea summer hydrography and submarine permafrost state, *Bull.*  
481 *Nov. Comp. Center* **15**, 13-22.
- 482 Gutjahr O., Heinemann G., Preußner A., Willmes S. & Drüe C. (2016) Quantification of ice  
483 production in Laptev Sea polynyas and its sensitivity to thin-ice parameterizations in a regional  
484 climate model, *The Cryosphere* **10**, 2999–3019.
- 485 Holmes R.M., McClelland J.W., Tank S.E., Spencer R.G.M. & Shiklomanov A.I. (2018) Arctic  
486 Great Rivers Observatory. Water Quality Dataset. Version 20181010.  
487 <https://www.arcticgreatrivers.org/data>
- 488 Huntley D.A., Leeks G.J.L. & Walling D. (2009) From rivers to coastal seas: the background  
489 and context of the land-ocean interaction study. In: Land-Ocean Interaction (Huntley D.A.,  
490 Leeks G.J.L., Walling D., eds), IWA Publ. House, London, UK, pp. 1-8.
- 491 Kane D.L., Yoshikawa K. & McNamara J.P. (2013) Regional groundwater flow in an area  
492 mapped as continuous permafrost, NE Alaska (USA), *Hydrogeology J.*, **21(1)**, 41-52.

493 Kirillov S.A. (2006) Spatial variation in sea-ice formation-onset in the Laptev Sea as a  
494 consequence of the vertical heat fluxes caused by internal waves overturning, *Polarforschung*  
495 **76(3)**, 119-123.

496 Lammers R.B., Pundsack J.W. & Shiklomanov A. (2007) Variability in river temperature,  
497 discharge and energy flux from the Russian pan-Arctic landmass, *J. Geophys. Res.* **112**, G04S59,  
498 doi: 10.1029/2006JG000370.

499 Liu B., Yang D. (2011) Siberian Lena River heat flow regime and change, IAHS Publ. 346, 71-  
500 76.

501 Magritsky D.V. (2016) Factors and trends of the long-term fluctuations of water, sediment and  
502 heat runoff in the lower reaches of the Lena River and the Vilyui River, *Bull. Moscow State*  
503 *University, Series 5 Geography*, **No. 6**, 85–94 (in Russian).

504 Magritsky D., Alexeevsky N., Aybulatov D., Fofonova V. & Gorelkin A. (2017) Features and  
505 evaluations of spatial and temporal changes of water runoff, sediment yield and heat flux in the  
506 Lena River delta, *Polarforschung* **87(2)**, 89-110.

507 Mangiafico S. (2019) ‘rcompanion’: Functions to support extension education program  
508 evaluation.

509 Nummelin A., Ilicak M., Li C. & Smedsrud S.H. (2016) Consequences of future increased Arctic  
510 runoff on Arctic Ocean stratification, circulation and sea ice cover, *J. Geophys. Res.* **121(1)**, 617-  
511 637.

512 Park H., Yoshikawa Y., Yang D. & Oshima K. (2017) Warming water in Arctic terrestrial rivers  
513 under climate change, *J. Hydromet.* **18(7)**, 1983-1995.

514 Pinneker Ye.V. (1990) Groundwater monitoring and management in permafrost areas, IAHS  
515 Publ. 173, 39-44.

516 Reinberg A.M. (1938): Hydrology of Soviet Arctic Rivers: Hydrology information about Lena,  
517 Ebitiem, Indigirka, Hatanga, Yenisei and Kolyma Rivers. *Proceed. Arctic Antarctic Res. Institute*  
518 **105**, 51-72 (in Russian).

519 RStudio: Integrated Development Environment for R (version 1.1.447). Computer Software,  
520 Boston, VA, USA (Retrieved 1 April 2019).

- 521 St. Jacques, J. M., Sauchyn D.J. (2009), Increasing winter baseflow and mean annual streamflow  
522 from possible permafrost thawing in the Northwest Territories, Canada, *Geophys. Res. Lett.*  
523 **36(1)**, L01401, doi: 10.1029/2008GL035822.
- 524 van Vliet M.T.H., Franssen W.H.P., Yearsley J.R., Ludwig F., Haddeland I., Lettenmaier D.P. &  
525 Kabat P. (2013) Global river discharge and water temperature under climate change, *Glob*  
526 *Environ Change* **23(2)**, 450-464, doi: 10.1016/j.gloenvcha.2012.11.002.
- 527 Wankiewicz A. (1984) Hydrothermal processes beneath Arctic river channels, *Wat. Resour. Res.*  
528 **20(10)**, 1417–1426.
- 529 Yang D., Liu B. & Ye B. (2005) Stream temperature changes over Lena River Basin in Siberia,  
530 *Geophys Res Lett* **32(5)**, L05401, doi: 10.1029/2004GL021568.
- 531 Yang D., Marsh P. & Ge S. (2014) Heat flux calculations for Mackenzie and Yukon Rivers,  
532 *Polar Science* **8(3)**, 232-241, doi: 10.1016/j.polar.2014.05.001.
- 533 Yang, D., X. Shi & Marsh P. (2015), Variability and extreme of Mackenzie River daily  
534 discharge during 1973–2011, *Quat. Int.*, **380–381**, 159–168, doi: 10.1016/j.quaint.2014.09.023.
- 535 Yoshikawa K.; Hinzman L.D. & Kane D.L. (2007) Springs and aufeis (icing) hydrology in  
536 Brooks Range, Alaska, *J. Geophys. Res.* **112**, G04S43, doi:10.1029/2006JG000294.
- 537 Zhang T., Barry R.G., Knowles K., Heginbottom G.A. & Brown J. (1999) Statistics and  
538 characteristics of permafrost and ground-ice distribution in the Northern Hemisphere, *Polar*  
539 *Geogr.* **23(2)**, 132-154.